Article

The effect of ozone and aerosols on erythemal irradiance in a low ozone event.

Raptis Ioannis-Panagiotis [1*], Eleftheratos Kostas [2] , Kazadzis Stelios [3], Kosmopoulos Panagiotis [1]

[1] Institute for Environmental Research and Sustainable Development, National Observatory of Athens, GR15236 Athens
[2] Faculty of Geology and Geoenvironment, University of Athens, Athens, Greece
[3] Physicalisch-Meteorologisches Observatorium Davos, World Radiation Center, CH-7260 Davos, Switzerland
* Correspondence: piraptis@noa.gr

Abstract: In this study we focus on measurements and modeled UV index at the region of Athens, Greece, during a period of a low ozone event. During the period of 12 to 19 of May 2020, total column ozone (TOC) showed extremely low values 35-55 DU (up to 15%) decrease from the climatic mean (being lower than the -2σ). This condition favors the increase of UV erythemal irradiance, since stratospheric ozone is the most important attenuator at the UVB spectral region. A parallel intrusion of Saharan Dust aerosols in the region has masked a large part of the low ozone effect on UV irradiance. In order to investigate the event, we have used spectral solar irradiance measurements from the Precision Solar Radiometer (PSR), total column ozone from the BREWER spectrophotometer and Radiative Transfer Model (RTM) calculations. Model calculations of UV Index (UVI) showed an increase of ~30% compared to the long term normal UVI due to the low TOC while at the same time and for particular days, aerosols masked this effect by ~20%. The study points out the importance of accurate measurements or forecasts of both ozone and aerosols when deriving UVI under unusual low ozone-high aerosol conditions.

Keywords: Ultraviolet; Ozone; Aerosol; UV Index; Erythemal; PSR;

1. Introduction

Ultraviolet (UV) radiation is a small part (~3% [1]) of the incoming solar radiation at Earth's surface but has a number of biological effects when absorbed by human skin, which can be either harmful or beneficial [2,3]. Harmful effects, linked to UV overexposure, include the skin erythema, the increased risk of skin cancer and multiple eye diseases (snow blindness, cataract). On the other hand, UV-B radiation, is extremely important for the human body, as it is crucial for synthesizing Vitamin D [5,6]. The effect of UV radiation on living cells is estimated by biological effective irradiances and doses [6]. Effective irradiances are retrieved by weighting actual spectral irradiances using the relative action spectrum. Doses are derived afterwards, when weight functions are integrated by time. UVI has been introduced by the World Meteorological Organization (WMO) in 1994, aiming to better inform the general public about the dangers of UV radiation [7]. UVI is a scaled version of erythemally-weighted UV, which is interpreted in an easily understandable scale of 0-20 and characterizes the safe exposure according to skin type ([8,9]. There is a growing concern in the scientific community on the variation of UV radiation in response to climate change [10-12]. Bais et al. [11] showed that higher values of UV are expected by the end of 21st century in tropical areas and a decrease in mid latitudes, but these estimations still hold high uncertainties. Eleftheratos et al., [13] showed that solar UVB irradiance that produces DNA damage would increase after the year 2050 due to the evolution of greenhouse gases in the future, thus suggesting that the process of climate change will overwhelm the effect of ozone recovery on UV-B irradiance in the mid latitudes.

UV irradiance reaching Earth's ground level is related to a number of factors and it is crucial to investigate them in order to monitor and predict it. In the UVB region O_3 and SO_2 are the main absorbers, while NO_2 is the dominant absorber at UVA [14]. Significant UV increase had been reported in the past decades due to ozone depletion [15]. Signs of recovering ozone, since Montreal Protocol was applied, has been recorded [16,17]. Nevertheless, extremely low values, which result in high UV, are measured occasionally.

Aerosols in the atmosphere, play also a crucial role to UV irradiance reaching Earth's surface. Aerosol optical depth (AOD) is a parameter that quantifies the attenuation of irradiance when passing from an aerosol layer and is wavelength dependent [18]. Different aerosol types have various effects in the UV, causing a spectral dependence of the extinction. Dust of desert origin has been reported as having the most significant extinction at the UV spectral region, which could have a major influence at the received UV irradiance, even eliminating the influence of low ozone, during severe events [19]. Additionally, Roman [20] has reported that desert dust could add an attenuation up to 50% in the direct UV irradiance, while the diffuse irradiance could increase up to 40%. Other aerosol types that have a significant role in the UV spectral region are black [21] and brown carbon [22]. Dust intrusions in the Eastern Mediterranean including Athens area have been presented in several studies [23-25].

The attenuators described above, are less important, when clouds are present, since clouds strongly attenuate all radiation, including UV. The increase of sun elevation proportionally increases the UV intensity. Main diurnal and seasonal cycles of UV are determined by the position of the sun, which is defined by astronomical calculation of the sun elevation, which is usually parameterized using Solar Zenith Angle (SZA), indicating of the air mass the light pass through [26]. UV irradiance also increases with altitude [27].

A number of studies have focused on the UV trends over the last decades, which are affected by trends in gases, aerosols and cloud coverage. Increase of UV has been reported in south and central Europe and decrease at higher latitudes [28]. Zerefos et al. [17] showed that the increase of total O_3 over the 1995-2006 period at mid-latitudes was not sufficient to reverse UVB increase, which was masked by decreasing aerosols. While Eleftheratos et al., [29] showed that at high latitudes, ozone increase and UVB decrease were in agreement in the absence of large aerosol variations.

UVI is currently monitored by about 160 stations from 25 countries around Europe [30]. Instruments operating at these stations are separated at three types, according to the technique of measurement, as broadband, narrow band filter and narrowband spectral radiometers. The estimated relative uncertainty for these UV irradiance radiometric measurements is 4.6 % [31], which propagates an uncertainty of 0.61 (at 1σ) for retrieved UVI [32]. Additionally, UV is monitored through satellite retrievals, which are covering the whole globe [33]. Satellite measurements are usually used for climatological studies [34] and for monitoring UV irradiance in areas with no ground based measurements. UVI is also routinely forecasted by a number of services and the output is provided to the general public for protection from the harmful UV doses. For example, the Tropospheric Emission Monitoring Internet Service (TEMIS), by the Royal Netherlands Meteorological Institute, provide a daily clear sky UVI forecast for Europe, for 8 days ahead, using the algorithm of Allart et al. [35], which takes into account TOC and SZA and uses an empirical aerosol correction, which leads to overestimations, when high aerosol loads are present [36].

In this study we focus on measurements and modeled UV index at the region of Athens, Greece, during a period of an extremely low ozone event. At this period TOC was much lower than the long term mean (in the range of 35-55 DU), reaching values as low as the -2σ values of the climatological average. A parallel invasion of Saharan Dust in the region has eliminated a large part of the low ozone effect on the UV irradiance. In order to investigate the event, we have used measurements from Precision Solar Radiometer (PSR) and BREWER spectrophotometer alongside with Radiative Transfer Model (RTM) simulations of the atmospheric conditions.

Besides the description of the observed extremely low ozone – high UVI – high aerosol Saharan dust event which we target in this study, it is important to highlight the motivation of this study and its difference from other works. The observed low ozone concentrations that occurred during May 2020 in Athens is a rare phenomenon, as May is largely characterized by high amounts of ozone transported from the tropics by the Brewer-Dobson circulation. These low ozone amounts contributed to high amounts of UVB irradiance in May, the magnitude of which is typically measured during July under cloudless conditions. It might be that such low ozone events become more frequent in the future during spring. In this respect it is important to know how much change in UVB radiation can be caused so that we can use this information to evaluate future calculations of UVB variability. At the same time, a Saharan dust intrusion occurred, altering the UVB radiation field. While UVB models predicted high levels of ultraviolet radiation in Athens during the low ozone week, the measured UVI levels were lower than expected. The reason for this was the increased dust aerosols that attenuated the incoming solar radiation reaching the ground. Model calculations for forecasting UVI currently used to inform the authorities and the general public, does not take into account the nature of Aerosols and the expected loads (e.g. TEMIS).

The occurrence of increased aerosols in May 12-19, 2020 in Athens, Greece, was expected to have a beneficial effect on the increased UVB radiation due to the extremely low ozone concentrations. It is shown that the increased aerosols balanced the effect of low ozone amounts on UVB irradiance, thus mitigating the enhanced UVB levels. The coincidence of increased aerosols and extremely low ozone during the week of May 12-19, 2020 in Athens, Greece, motivated us to study this peculiar event and to better quantify the roles of dust aerosols and ozone on UVB irradiance. The paper is organized as follows. The data sources (ground-based instruments, satellite data, modelling) and methodology are described in Section 2. The abnormal ozone, UVI and AOD measurements during the exceptional week of May 2020 in Athens and the respective climatological values are presented in Section 3. Finally, Section 4 summarizes the main results.

2. Data

Data used in this study were recorded at two different locations in Athens, Greece by PSR and Brewer instruments. The two locations are 5 km apart. The Brewer is installed at the roof of Biomedical Research Foundation of the Academy of Athens, which is located in a green area at a distance of about 4 km from the city center and is partly influenced by urban emissions. The PSR is installed at the Actinometric Station of National Observatory of Athens, in a green area in the city center. Aerosols in Athens can consist of sea-salt aerosols, dust from Sahara desert, smoke particles from forest fires, and small particles typical of urban and industrialized environments [37-39].

2.1 PSR

The Precision Solar Spectroradiometer has been designed and manufactured by PMOD/WRC, Davos, Switzerland, aiming high precision and accuracy for solar spectral measurements. It measures irradiance at 1024 channels in the spectral range of 300-1020nm with an average step of ~0.7nm, spectral resolution in the range of 1.5 to 6nm (according to measured wavelength) [40]. PSR 007 is installed in Athens (37.9N 23.7E, 130 m above sea level) and it was last calibrated on June 2019 at the world radiation center using a calibrated standard 1000W tungsten-halogen FEL lamp. Uncertainty of measurements has been estimated in the range of 1.7-2.0%, with higher uncertainties recorded at the UV spectral region, due to lower signal and stray light [41]. PSR 007 has a global sensor mounted on the auxiliary port and by using the built in shutter of the instrument, Global Horizontal Irradiance (GHI) and direct irradiance can be measured, by the same spectrometer. Thus, the same calibration and uncertainty budget is applied. The spectral measurement frequency is 1 minute.

UV Index is the parameter retrieved from PSR measurements, used in this study. The formula for the calculation is

$$UVI = k_{er} \int_{\lambda_1}^{\lambda_2} E_\lambda \, s_{er}(\lambda) d\lambda \quad (1)$$

Where k_{er} is a constant equal to 40 W/m², E_λ is the recorded solar spectral irradiance at wavelength λ, $S_{er}(\lambda)$ is the erythema action spectrum [42] and λ_1 and λ_2 are the limits of the UV spectral region. For our case the integrated spectral region is 300 to 400nm. This approach has an advantage, compared to broadband based measured UVIs, since the whole spectrum of the region 300-400nm is recorded and no additional corrections are needed [32].

2.2 The Brewer spectrophotometer

In this study we analyze TOC, UV irradiance and AOD retrievals from a Brewer MKIV spectrophotometer (number #001) operating at the roof of the Biomedical Research Foundation of the Academy of Athens in Greece (38.0 N, 23.8 E, 180 m a.s.l) since 2004. The Brewer is an automated, diffraction-grating spectrometer that provides observations of the sun's intensity in the near UV range. The instrument measures the intensity of radiation in the UV absorption spectrum of ozone at five wavelengths (306.3, 310.1, 313.5, 316.8 and 320.1 nm) with a resolution of 0.5 nm. These data are used to derive columnar ozone and sulfur dioxide amounts and the aerosol optical depth [43].

Measurements with the Brewer #001 have been exploited in several studies analyzing columnar ozone, sulfur dioxide and aerosol optical depth [44-47]. TOC analyzed in this study is calculated from a combination of direct sun (DS) measurements at UV wavelengths that experience different absorption by ozone passing through the atmosphere (310.1, 313.5, 316.8 and 320.1 nm), weighted with a predefined set of constants chosen to minimize the influence of SO_2 and linearly varying absorption features from, e.g., clouds or aerosols [48]. TOC is retrieved using the differential absorption method [49].

The Brewer #001 was regularly recalibrated against the traveling standard Brewer instrument #017 in 2002 in Thessaloniki and in 2004, 2007, 2010, 2013 and 2019 on site in Athens. Internal standard lamp tests are performed on a daily basis to detect possible instrumental drifts. Ozone data are recalculated after standard lamp test corrections and are analyzed using the O3Brewer data management software [50].

Finally, the AOD analysed in this study is retrieved from DS measurements at 5 standard wavelengths (306.3, 310.1, 313.5, 316.8, 320.1 nm) using the O3baod software package developed by Martin Stanek (http://www.o3soft.eu/o3baod.html). The setup of the software for the Athens Brewer was done with the assistance of M. Stanek (private communication). AOD at 320.1 nm is reported here.

2.3 Satellite data

Satellite data have been used in order to provide further evidence on the range of TOC. UV satellite record started in 1978 with Total Ozone Mapping Spectrometer (TOMS) and continued until today with Ozone Monitoring Instrument (OMI), which is nadir-viewing UV/visible backscatter spectrometer on-board NASA's satellite Aura. The OMI ozone product algorithm and the TOC retrieving process is described in Bhartia and Wellemeyer [51].The main procedures include a fitting of ozone absorption cross-section to the measured spectrum, an estimation of air mass factor and corrections for clouds effects. Data processing and quality assurance of the TOC product is analytically outlined at Veefkind et al. [52]. OMI TOC retrieval has one overpass above Athens per day in a distance less than 50km since 2002, which could be used to create an almost two decades long timeseries. Copernicus Atmospheric Service (CAMS) provide a reanalysis database of TOC, which we also used to detect the general ozone circulation at the area at the time of the event. This database is assimilating data from different satellites (SBUV/2, OMI, SCIAMACHY, GOME, MIPAS, MLS, GOME-2) alongside with chemical transport modelling to provide TOC at 0.4ºX0.4º spatial grid [53].

2.4 Radiative transfer model

Radiative Transfer calculations using the Libradtran package [54-55] has been performed, aiming to simulate the atmospheric conditions and evaluate forecasts using different input variables. In particular, different set-ups of the code have been run, using climatological AOD and TOC values, and daily measured AOD and TOC values. Single Scattering Albedo (SSA) was set to climatological value of 0.9, but during dust event SSA was set to more representative value of 0.86 for these type of aerosol in the UV spectral region [56,57]. Output of the run was GHI at 300-400 nm at spectral resolution of 0.1 nm. Corresponding UVI was calculated by applying the erythema action spectrum to the output spectra using equation (1).

3. Results and discussion

Figure 1 shows the long term variability of TOC in Athens, as retrieved from Brewer in the period 2004-2019. Ranges of 1 and 2 σ around the mean daily value are highlighted. Retrievals of 2020 are also shown and the period of the extreme low ozone event is found between 12 and 19 May. The mean TOC for the region, for May is 346±16 DU, while for this week it dropped down to 280-295 DU. The seasonal variation, follows the mid latitude behavior of Stratospheric Ozone, having maximum values during late winter-early spring and lower values at the end of summer and in autumn. As a threshold to characterize an extreme event, we have used the 2σ of the climatology. In a theoretical normal distribution, 95.5% of the values would have been in this range. This corresponds to ~1 day per month outside these limits. Thus, a period of 9 consecutive days below the limit has very low possibility of occurring. Although, the actual distribution of the values has some deviation from a theoretical normal distribution, it is safe to characterize this period as very rare low ozone event for the region.

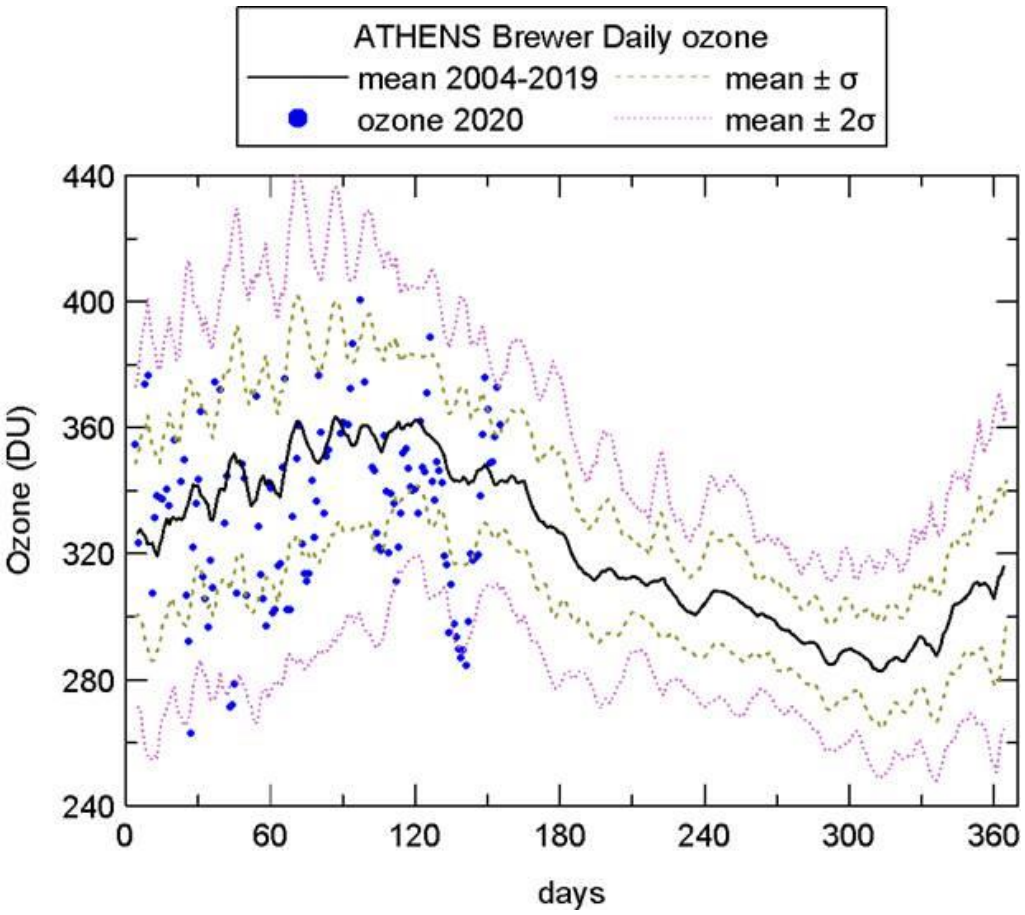

Figure 1. Average TOC at Athens, retrieved by Brewer, for the period 2004-2019, per day, along with 1 and 2 σ variations, and values retrieved in 2020.

In order to understand the negative anomaly of TOC, maps of the greater area around Athens, Greece for 12 and 16 May, are presented in figure 2, as an example of the concentrations in the area. The anomaly could be triggered either by a local tropospheric airmass ascend in the stratosphere or the intrusion of tropical stratospheric air mass. The picture of TOC in the area, during the event, shows that the zonal spatial distribution scheme [58] is broken by an intrusion from lower latitudes, which makes the transport of tropical air the most probable cause. These intrusions are mainly generated by gravitational waves [59]. Butchart et al. [60] have analyzed different models and measurements for the meridional variation of Ozone and concluded that under expected climatic changes, this kind of events will be more frequent. Hence, large TOC negative anomalies could be a major issue at mid-latitudes in the near future.

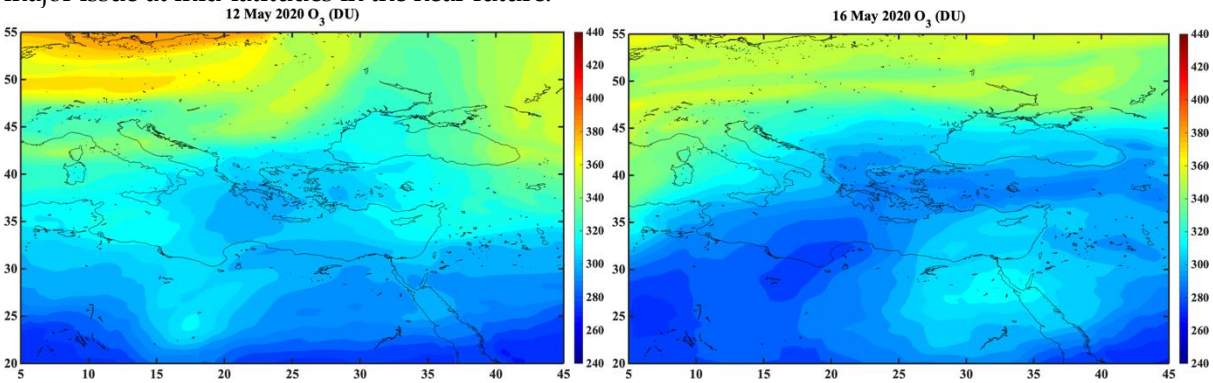

Figure 2. Spatial variability of TOC around Northern Africa, Middle East and Europe for 12 and 16 May 2020, as retrieved by CAMS.

Figure 3 shows the variation of UVI, TOC and AOD during May 12-19, 2020, as retrieved by the corresponding instruments. UVI is retrieved from PSR measurements. Higher UVI was recorded on 19 May, when maximum value was 9.2. All the day after 13 May has maximum UVI higher than 7.9. On May 12, there were frequent overcast cloud conditions, which appear in the form of broken curves in the UVI retrieval. TOC from both BREWER and OMI was constantly below the 2σ of the climatological mean during the whole period. Lowest values are reported on 16 and 17 May. AOD is well below the climatological mean on May 13, and in the evening, an intrusion of Saharan dust reaches Athens and very high values are recorded from 14 to 17 of May. On the last days AOD reduces and approaches the mean climatological values. For May 16-19, the UVI time series are sporadically affected by the presence of cirrus clouds. To avoid the effects of clouds, we selected to study further, days that were strictly cloud free based on PSR observations. Such cloudless conditions appear on May 13, 14 and 15. Based on all the above conditions the days 13 and 15 of May were selected to be more intensively studied, as representative of cloudless days of low ozone and low aerosols (13/5) and low ozone high aerosol (15/5). Data from 14/5 are later used to simulate the effects of low ozone and high AOD on UV spectra.

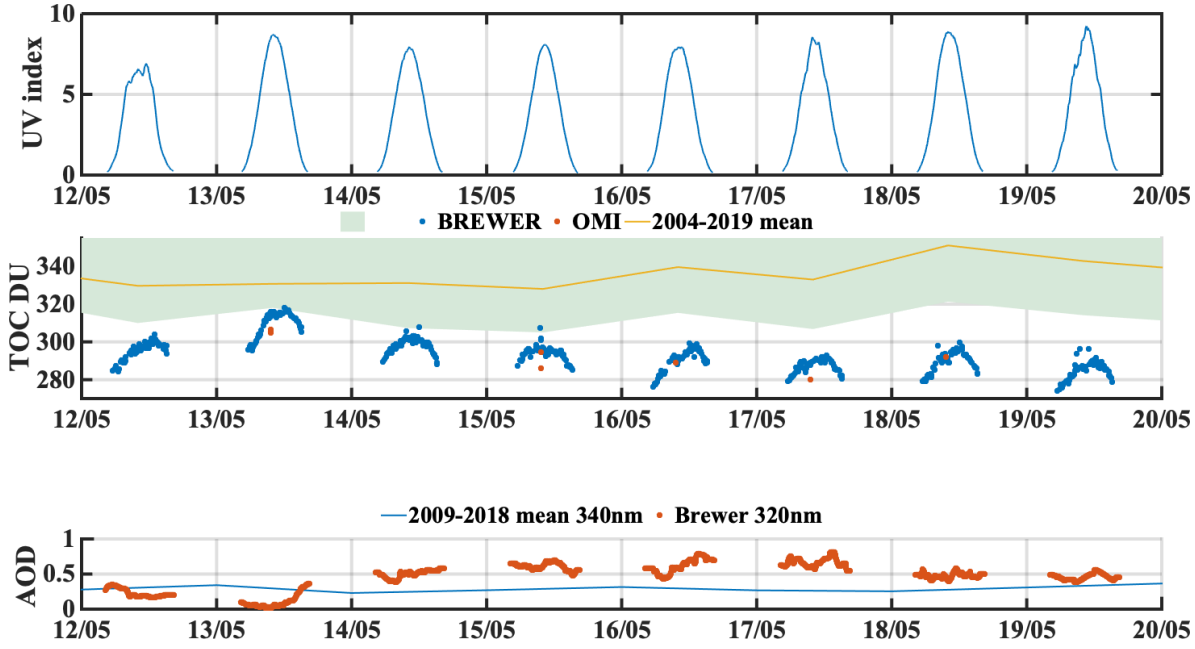

Figure 3. Variation of UVI as retrieved from PSR measurements (upper plot). Variation of TOC as retrieved from Brewer compared to average and average±2σ for the period, derived from Brewer 2004-2019 data (middle plot). AOD at 320nm as retrieved from Brewer along with climatological average AOD at 340 nm as retrieved from AERONET for the period 2009-2018 [39].

Figure 4 shows UVI retrieved from PSR on May 13, alongside with RTM simulations of UVI estimated with climatological TOC and AOD and BREWER's AOD and TOC values. PSR retrieved UVI is up to 11.2% (0.92 UVI) higher than the theoretical simulated with climatological TOC and AOD inputs. Using measured AOD and TOC the agreement with the PSR has an R^2=0.98 and a mean bias error MBE=0.11. Hence, the observed deviation from the theoretical climatological UVI can be explained by the variation of TOC and AOD. Mean AOD for the day is 0.22 (33.2%) lower than the climatological value and mean TOC is 32 DU lower (9.4%) respectively. Both these factors are contributing to higher UVI. Higher differences are observed around local noon, when UVI has maximum values. For a large part of the day, absolute UVI differences are small and start to

differentiate when UVI is higher than 5. The following days, later in the week, had even lower ozone values, but not all of them were cloud free and none of them had low AOD values. Maximum values of UVI are the ones usually reported to the general public and are the ones with the highest differences.

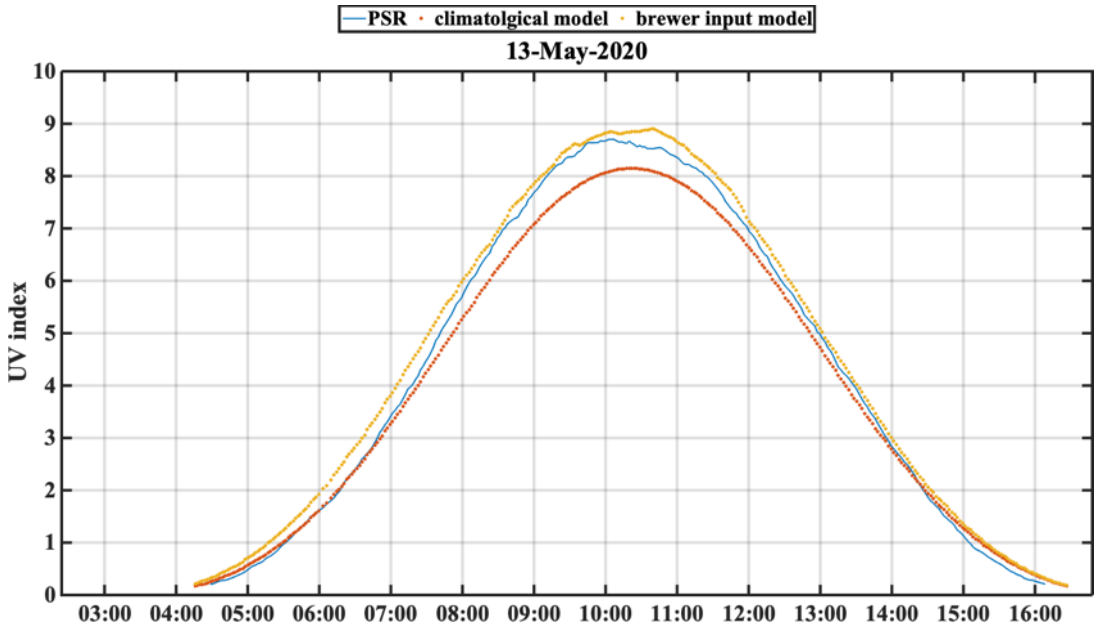

Figure 4. Diurnal variation of UVI on May 13, 2020 as retrieved from PSR measurements (blue curve), in comparison with theoretical UVI predicted using RTM with climatological TOC and AOD inputs (orange dots) and modeled UVI using brewer AOD and TOC as input (yellow dots).

On 15 May 15, mean ozone was 43 DU lower than the climatological value. Purple curve on figure 5 shows the theoretical UVI calculated with this TOC value but with 0 aerosols. Ozone at so low range could lead to an increase of up to 28.5% of UVI (2.1 UVI), compared to the climatological estimations. On the other hand, mean AOD on this day was 0.31 (46.7%) higher than the climatological mean, which leads to a decrease of UVI. As shown on figure 5, simulation of UVI with climatological and measured TOC and AOD values are almost identical (R^2=0.99 and MBE=0.04). PSR retrieved UVI also agrees with these simulations (R^2=0.99 and MBE=0.06). Hence, the two events have opposite effect on UVI, eliminating each other, leading to conditions similar to the climatological simulation. We should conclude here, that neglecting either effect of ozone or aerosols, could lead to significant misestimation to UVI and erroneous recommendations to the general public.

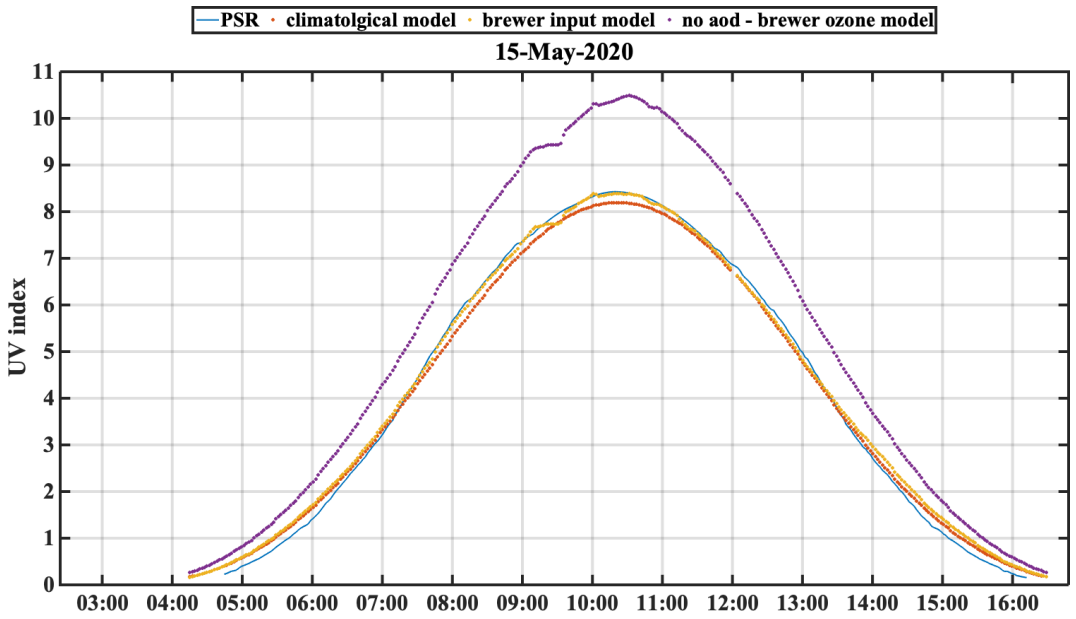

Figure 5 Diurnal variation of UVI on May 15, 2020 as retrieved from PSR measurements, in comparison with theoretical UVI predicted using RTM with climatological TOC and AOD inputs , modeled UVI using Brewer AOD and TOC as input and modeled UVI using Brewer TOC but zero aerosols.

At figure 6, theoretical spectra at SZA of 30º and 60º are divided, from two separate RTM runs, using a constant climatological AOD (0.3) and different TOC; climatological (335 DU) and measured (292 DU as average for the 14th of May). At wavelengths higher than 330 nm, the ratio is constantly 1, where ozone has almost zero influence. At lower spectral regions, the ratio becomes ~1.5 at 305 nm and towards the lower wavelength regions the ratios became higher exponentially. It is clear from this figure, that UVA region is practically insensitive to TOC changes, UVB is highly sensitive and as it compromises the most important part for erythema, it is the region that affects more the UVI. The average effect in the UVB region is a 32% increase in irradiance. This could lead to 29% increase in the estimated UVI. The ratios depend on the SZA, as higher SZA's correspond to higher ozone attenuation thus higher ratios.

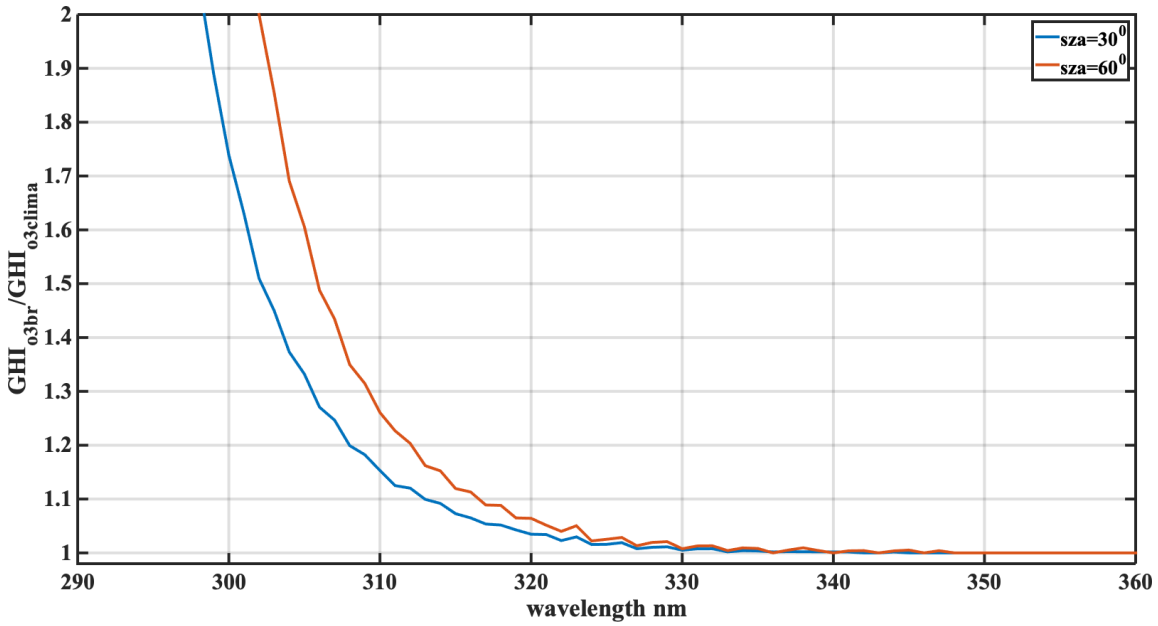

Figure 6 Ratio of theoretical spectra in the UV region, as derived from RTM, with mean TOC measured by Brewer on May 14, 2020, and climatological TOC, at two Solar Zenith Angles.

At figure 7, theoretical spectral ratios of GHI simulated with AOD=0.5 (14 May) and AOD=0 at SZA=30 ºand 60º are presented. In all the above runs, TOC was set to the same climatological values (335 DU). These ratios are less spectral depended and their absolute value depends on the AOD while their spectral change by the spectral characteristics of the aerosols (Ängström exponent). Variation of the ratio, when SZA is 30º, is from 0.73 at 300 nm to 0.82 at 400nm. When SZA is higher, the attenuation due to aerosols is higher. Thus, the difference due to aerosols, is very similar in UVA and UVB regions. AOD at 0.5, causes about 25% drop to the solar UV irradiance, which leads to decrease of 28% at UVI. We should also highlight the importance of SSA in the calculations, since the type of the aerosols affects significantly the scattering characteristics of radiative transfer; hence, the GHI ratios will vary accordingly. We remind that SSA was set to 0.86 for the dust aerosols according to section 2.4.

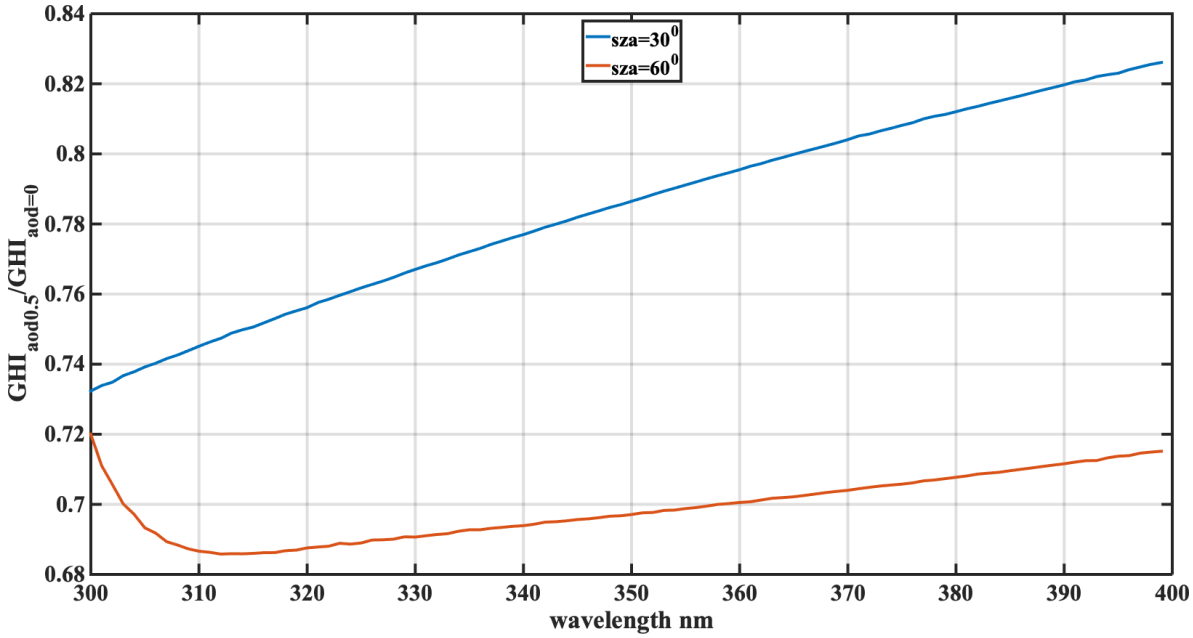

Figure 7 Ratio of theoretical spectra in the UV region, as derived from RTM, with mean AOD measured by Brewer on May 14, 2020 and no aerosols, at two Solar Zenith Angles.

4. Summary

During May 12-19, 2020 an extreme low TOC event was observed over Athens area. TOC was lower than the climatological average (- 2σ) for the whole week period. In addition, during some days AOD values were lower than the climatological average, while on other days a dust aerosol intrusion was linked with AOD values almost double than the May average for Athens. Our analysis is confined to days that were strictly cloud free in order to avoid the effect of cloudiness and study the effects of ozone and aerosols on the UV spectra.

On the 15th of May that was with a day with very low TOC and the highest AOD, theoretical calculations showed that TOC variation alone could cause an increase of ~30% in the UVI compared with the climatological average. However, aerosol presence masked ~20% of this increase as the dust intrusion lead to much higher than normal AOD values.

Through RTM calculations, we have estimated that at 305 nm, when SZA is 30º, GHI compared to the one with average AOD and TOC, will be 26% lower due to aerosols and 34% higher due to TOC decrease, while at 60º SZA aerosols will attenuate GHI by 31% and ozone will increase it by 59%. Accordingly, at 325 nm, aerosols will cause 24% and 31% drop of GHI, at 30º and 60º SZA, while

ozone will increase it by 2% at both SZA. We highlight that these estimates were derived using measurements at May14th, 2020 a cloud free day with AOD of 0.5 and mean daily ozone of 292 DU.

This study is investigating the parallel effects of factors affecting a health-related parameter such as the UVI. When studying the UVI dependence of TOC and AOD it is important to focus on the different spectral regions, as Ozone acts mainly in the UVB region, which also determines the largest part of UVI. Aerosols act more uniformly in the whole UV region and their spectral response is determined by the Ångström exponent. It should also be highlighted, that ignoring day to day changes on either O_3 or aerosols, when estimating UVI, could lead to very high errors. Simultaneously occurring events that could mutually eliminate their effects are happening occasionally and having better knowledge on all these parameters will lead to better forecasting of UVI.

The case presented here is a demonstration of the combined effects of TOC and aerosols. Changes in UVI under very low TOC events can be masked by high aerosol loads. Even if TOC is the major parameter affecting UVI, in this event, we saw that a moderate to high dust intrusion eliminated completely the very low TOC effect to the incoming UVI. Our findings demonstrate that aerosols in the UV region are very important and their optical properties (especially in the UVB) have to be accurately known in order to simulate the UVI and inform the public objectively in the absence of accurate UV measurements.

Acknowledgements

We acknowledge support and funding of this work by the project "Panhellenic Infrastructure for Atmospheric Composition and Climate change" (MIS 5021516) which is implemented under the action "Reinforcement of the Research and Innovation Infrastructure", funded by the Operational Program "Competitiveness, Entrepreneurship and Innovation" (NSRF 2014–2020) and co-financed by Greece and the European Union (European Regional Development Fund).The research work was also partially supported by the Hellenic Foundation for Research and Innovation (H.F.R.I.) under the "First Call for H.F.R.I. Research Projects to support Faculty members and Researchers and the procurement of high-cost research equipment grant" (Project Number: 300).

References

1. Solar Spectra by National Renewable Energy Laboratory of United States, https://www.nrel.gov/grid/solar-resource/spectra.html, Access date 2/9/2020
2. Juzeniene, A., Brekke, P., Dahlback, A., Andersson-Engels, S., Reichrath, J., Moan, K., Holick, M. F., Grant, W. B. and Moan, J.: Solar radiation and human health, *Reports Prog. Phys*.,**2011**, 74(6), doi:10.1088/0034-4885/74/6/066701.
3. Lucas, R., McMichael, T., Smith, W. and Armstrong, B.: Solar Ultraviolet Radiation: Global burden of disease from solar ultraviolet radiation., *Environmental burden of disease series* **,2006** , 13.
4. Webb, A. R., Kift, R., Berry, J. L. and Rhodes, L. E.: The vitamin D debate: Translating controlled experiments into reality for human sun exposure times, *Photochem. Photobiol*., **2011**, 87(3), 741–745, doi:10.1111/j.1751-1097.2011.00898.x.
5. Webb, A. R. and Engelsen, O.: Calculated Ultraviolet Exposure Levels for a Healthy Vitamin D Status, *Photochem. Photobiol*. **, 2006**, 82(6), 1697, doi:10.1562/2006-09-01-ra-670.
6. McKenzie, R., Blumthaler, M., Diaz, S., Fioletov, V. E., Herman, J. R., Seckmeyer, G., Smedley, A. R. D. and Webb, A. R.: Rationalizing nomenclature for UV doses and effects on humans. **, 2014**, CIE and WMO-GAW Joint Report; 2014. Report No. CIE 209:2014
7. WMO: Report of the WMO Meeting of Experts on UV-B Measurements, Data Quality and Standardization of UV Indices, 1994., **1995**.
8. WHO et al.: Global Solar UV Index: A Pratical Guide, No. WHO/SD., Geneva, Switzerland., **2002**.
9. Fioletov, V., Kerr, J.B. and Fergusson, A. The UV index: definition, distribution and factors affecting it. *Canadian journal of public health***., 2010**, *101*(4), pp.I5-I9.
10. Bais, A. F., Lucas, R. M., Bornman, J. F., Williamson, C. E., Sulzberger, B., Austin, A. T., Wilson, S. R., Andrady, A. L., Bernhard, G., McKenzie, R. L., Aucamp, P. J., Madronich, S., Neale, R. E., Yazar, S., Young, A. R., De Gruijl, F. R., Norval, M., Takizawa, Y., Barnes, P. W., Robson, T. M., Robinson, S. A.,

Ballaré, C. L., Flint, S. D., Neale, P. J., Hylander, S., Rose, K. C., Wängberg, S., Häder, D. P., Worrest, R. C., Zepp, R. G., Paul, N. D., Cory, R. M., Solomon, K. R., Longstreth, J., Pandey, K. K., Redhwi, H. H., Torikai, A. and Heikkilä, A. M.: Environmental effects of ozone depletion, UV radiation and interactions with climate change: UNEP Environmental Effects Assessment Panel, update 2017, *Photochem. Photobiol. Sci.* **, 2018**, 17(2), 127–179, doi:10.1039/c7pp90043k.

11. .Bais, A. F., Bernhard, G., McKenzie, R. L., Aucamp, P. J., Young, P. J., Ilyas, M., Jöckel, P. and Deushi, M.: Ozone-climate interactions and effects on solar ultraviolet radiation, *Photochem. Photobiol. Sci.* **, 2019**, 18(3), 602–640, doi:10.1039/C8PP90059K.
12. McKenzie, R. L., Aucamp, P. J., Bais, A. F., Björn, L. O., Ilyas, M. and Madronich, S.: Ozone depletion and climate change: impacts on UV radiation, *Photochem. Photobiol. Sci*. **, 2011**, 10(2), 182, doi:10.1039/c0pp90034f.
13. Eleftheratos, K., Kapsomenakis, J., Zerefos, C.S., Bais, A.F., Fountoulakis, I., Dameris, M., Jöckel, P., Haslerud, A.S., Godin-Beekmann, S., Steinbrecht, W. and Petropavlovskikh, I.,. Possible Effects of Greenhouse Gases to Ozone Profiles and DNA Active UV-B Irradiance at Ground Level. *Atmosphere*, **2020,***11*(3), p.228.
14. Bais, A. F., Zerefos, C. S., Meleti, C., Ziomas, I. C. and Tourpali, K.: Spectral measurements of solar UVB radiation and its relations to total ozone, SO2, and clouds, *J. Geophys. Res*. **, 1993**, 98(D3), 5199–5204, doi:10.1029/92JD02904.
15. Kerr, J. B. and McElroy, C. T.: Evidence for large upward trends of ultraviolet-B radiation linked to ozone depletion, *Science*., **1993,** 262(5136), 1032–1034, doi:10.1126/science.262.5136.1032.
16. Kuttippurath, J. and Nair, P. J.: The signs of Antarctic ozone hole recovery, *Sci. Rep*. **, 2017**, 7(1), 1–8, doi:10.1038/s41598-017-00722-7.
17. Zerefos, C. S., Tourpali, K., Eleftheratos, K., Kazadzis, S., Meleti, C., Feister, U., Koskela, T. and Heikkilä, A.: Evidence of a possible turning point in solar UV-B over Canada, Europe and Japan, *Atmos. Chem. Phys*.**, 2012,** 12(5), 2469–2477, doi:10.5194/acp-12-2469-2012.
18. Kazadzis, N. Kouremeti, A. Bais, A. Kazantzidis and C. Meleti, Aerosol forcing efficiency in the UVA region from spectral solar irradiance measurements, *Ann. Geophys*., **2009**, 27, 2515–2522
19. Di Sarra, A., Cacciani, M., Chamard, P., Cornwall, C., DeLuisi, J.J., Di Iorio, T., Disterhoft, P., Fiocco, G., Fua, D. and Monteleone, F., Effects of desert dust and ozone on the ultraviolet irradiance at the Mediterranean island of Lampedusa during PAUR II. *Journal of Geophysical Research: Atmospheres*, **2002**, *107*(D18), pp.PAU-2.
20. Román, R., Antón, M., Valenzuela, A., Gil, J.E., Lyamani, H., De Miguel, A., Olmo, F.J., Bilbao, J. and Alados-Arboledas, L., Evaluation of the desert dust effects on global, direct and diffuse spectral ultraviolet irradiance. *Tellus B: Chemical and Physical Meteorology*, **2013**, *65*(1), p.19578.
21. Barnard, W.F., Saxena, V.K., Wenny, B.N. and DeLuisi, J.J., Daily surface UV exposure and its relationship to surface pollutant measurements. *Journal of the Air & Waste Management Association*, **2003**,*53*(2), pp.237-245
22. Mok, J., Krotkov, N. A., Torres, O., Jethva, H., Li, Z., Kim, J., Koo, J. H., Go, S., Irie, H., Labow, G., Eck, T. F., Holben, B. N., Herman, J., Loughman, R. P., Spinei, E., Soo Lee, S., Khatri, P. and Campanelli, M.: Comparisons of spectral aerosol single scattering albedo in Seoul, South Korea, *Atmos. Meas. Tech*. **, 2018**, 11(4), 2295–2311, doi:10.5194/amt-11-2295-2018.
23. Papayannis, R.E. Mamouri, V. Amiridis, S. Kazadzis, C. Pérez, G. Tsaknakis, P. Kokkalis Systematic lidar observations of Saharan dust layers over Athens, Greece in the frame of EARLINET project (2004-2006) *Annales geophysicae***, 2009**, 27, 3611-3620
24. Kosmopoulos, P. G., Kazadzis, S., Taylor, M., Athanasopoulou, E., Speyer, O., Raptis, P. I., Marinou, E., Proestakis, E., Solomos, S., Gerasopoulos, E., Amiridis, V., Bais, A., and Kontoes, C.: Dust impact on surface solar irradiance assessed with model simulations, satellite observations and ground-based measurements, *Atmos. Meas. Tech*. **, 2017**, 10, 2435-2453, https://doi.org/10.5194/amt-10-2435-2017.
25. Solomos , S., Kalivitis, N., Mihalopoulos, N., Amiridis, V., Kouvarakis, G., Gkikas, A., Binietoglou, I., Tsekeri, A., Kazadzis, S., Kottas, M., Pradhan, Y., Proestakis, E., Nastos, P.T., Marenco, F.: From Tropospheric Folding to Khamsin and Foehn Winds: How Atmospheric Dynamics Advanced a Record-Breaking Dust Episode in Crete. *Atmosphere***, 2018**, 9, 240
26. Seckmeyer, G., Pissulla, D., Glandorf, M., Henriques, D., Johnsen, B., Webb, A., Siani, A. M., Bais, A., Kjeldstad, B., Brogniez, C., Lenoble, J., Gardiner, B., Kirsch, P., Koskela, T., Kaurola, J., Uhlmann, B., Slaper, H., Den Outer, P., Janouch, M., Werle, P., Gröbner, J., Mayer, B., De La Casiniere, A., Simic, S.

and Carvalho, F.: Variability of UV irradiance in Europe, *Photochem. Photobiol.* **, 2008**, 84(1), 172–179, doi:10.1111/j.1751-1097.2007.00216.x.

27. Blumthaler, M., Ambach, W. and Ellinger, R.: Increase in solar UV radiation with altitude, *J. Photochem. Photobiol. B Biol.* **, 1997**, 39(2), 130–134, doi:10.1016/S1011-1344(96)00018-8.
28. Fountoulakis, I., Diémoz, H., Siani, A. M., Laschewski, G., Filippa, G., Arola, A., Bais, A. F., Backer, H. De, Lakkala, K., Webb, A. R., De Bock, V., Karppinen, T., Garane, K., Kapsomenakis, J., Koukouli, M. E. and Zerefos, C. S.: Solar UV irradiance in a changing climate: Trends in europe and the significance of spectral monitoring in Italy, *Environ. - MDPI*, **2020**, 7(1), 1–31, doi:10.3390/environments7010001.
29. Eleftheratos, K., Kazadzis, S., Zerefos, C.S., Tourpali, K., Meleti, C., Balis, D., Zyrichidou, I., Lakkala, K., Feister, U., Koskela, T. and Heikkilä, A.. Ozone and spectroradiometric UV changes in the past 20 years over high latitudes. *Atmosphere-Ocean*, **2015,** *53*(1), pp.117-125.
30. Schmalwieser, A. W., Gröbner, J., Blumthaler, M., Klotz, B., De Backer, H., Bolsée, D., Werner, R., Tomsic, D., Metelka, L., Eriksen, P., Jepsen, N., Aun, M., Heikkilä, A., Duprat, T., Sandmann, H., Weiss, T., Bais, A., Toth, Z., Siani, A. M., Vaccaro, L., Diémoz, H., Grifoni, D., Zipoli, G., Lorenzetto, G., Petkov, B. H., Di Sarra, A. G., Massen, F., Yousif, C., Aculinin, A. A., Den Outer, P., Svendby, T., Dahlback, A., Johnsen, B., Biszczuk-Jakubowska, J., Krzyscin, J., Henriques, D., Chubarova, N., Kolarž, P., Mijatovic, Z., Groselj, D., Pribullova, A., Gonzales, J. R. M., Bilbao, J., Guerrero, J. M. V., Serrano, A., Andersson, S., Vuilleumier, L., Webb, A. and O'Hagan, J.: UV Index monitoring in Europe, *Photochem. Photobiol. Sci.*, **2017,** 16(9), 1349–1370, doi:10.1039/c7pp00178a.
31. Gröbner, J. and Sperfeld, P., Direct traceability of the portable QASUME irradiance scale to the primary irradiance standard of the PTB. *Metrologia*, **2005,** *42*(2), p.134.
32. Hülsen, G., Gröbner, J., Bais, A., Blumthaler, M., Diémoz, H., Bolsée, D., Diaz, A., Fountoulakis, I., Naranen, E., Schreder, J. and Stefania, F., Second solar ultraviolet radiometer comparison campaign UVC-II. *Metrologia*, **2020,** *57*(3), p.035001.
33. Verdebout, J.: A European satellite-derived UV climatology available for impact studies, *Radiat. Prot. Dosimetry***, 2004**, 111(4), 407–411, doi:10.1093/rpd/nch063.
34. Herman, J. R.: Global increase in UV irradiance during the past 30 years (1979-2008) estimated from satellite data, *J. Geophys. Res. Atmos.* **, 2010**, 115(4), doi:10.1029/2009JD012219.
35. Allaart, M., van Weele, M., Fortuin, P. and Kelder, H.: An empirical model to predict the UV-index based on solar zenith angles and total ozone, *Meteorol. Appl.*, **2004,** 11(1), 59–65, doi:10.1017/S1350482703001130.
36. Zempila, M. M., Koukouli, M. E., Bais, A., Fountoulakis, I., Arola, A., Kouremeti, N. and Balis, D.: OMI/Aura UV product validation using NILU-UV ground-based measurements in Thessaloniki, Greece, *Atmos. Environ.*, **2016,**140, 283–297, doi:10.1016/j.atmosenv.2016.06.009.
37. Gerasopoulos, E., Kokkalis, P., Amiridis, V., Liakakou, E., Perez, C., Haustein, K., Eleftheratos, K., Andreae, M. O., Andreae, T. W., and Zerefos, C. S.: Dust specific extinction cross-sections over the Eastern Mediterranean using the BSC-DREAM model and sun photometer data: the case of urban environments, *Annales Geophysicae***, 2009**, 27, 2903–2912.
38. Amiridis, V., Zerefos, C., Kazadzis, S., Gerasopoulos, E., Eleftheratos, K., Vrekoussis, M., Stohl, A., Mamouri, R., Kokkalis, P., Papayannis, A., Eleftheriadis, K., Diapouli, E., Keramitsoglou, I., Kontoes, C., Kotroni, V., Lagouvardos, K., Marinou, E., Giannakaki, E., Kostopoulou, E., Giannakopoulos, C., Richter, A., Burrows, J., and Mihalopoulos, N.: Impact of the 2009 Attica wild fires on the air quality in urban Athens, *Atmos. Environ.*, **2012,** 46, 536–544, doi:10.1016/j.atmosenv.2011.07.056.
39. Raptis, I.P., Kazadzis, S., Amiridis, V., Gkikas, A., Gerasopoulos, E. and Mihalopoulos, N., 2020. A Decade of Aerosol Optical Properties Measurements over Athens, Greece. *Atmosphere*, *11*(2), p.154.
40. Raptis, P.I., Kazadzis, S., Gröbner, J., Kouremeti, N., Doppler, L., Becker, R. and Helmis, C., Water vapour retrieval using the Precision Solar Spectroradiometer. *Atmospheric Measurement Techniques*, **2018,**11(2).
41. Gröbner, J. and Kouremeti, N., The Precision Solar Spectroradiometer (PSR) for direct solar irradiance measurements. *Solar Energy*, **2019**,185, pp.199-210.
42. Webb, A.R., Who, what, where and when—influences on cutaneous vitamin D synthesis. *Progress in biophysics and molecular biology***, 2006**, *92*(1), pp.17-25.

43. Kerr, J. B., McElroy, C. T., and Olafson, R. A.: Measurements of ozone with the Brewer ozone spectrophotometer, *Proceedings of the Quadrennial Ozone Symposium, Boulder, Colorado*, **1980** edited by: London, J., National Center for Atmospheric Research, Boulder, Colorado, 74–79.

44. Kazantzidis, A., Bais, A. F., Zempila, M. M., Meleti, C., Eleftheratos, K., and Zerefos, C.: Evaluation of ozone column measurements over Greece with NILU–UV multi–channel radiometers, *International Journal of Remote Sensing*, **2009,** Vol. 30, Nos. 15-16, 4273–4281, doi: 10.1080/01431160902825073.

45. Raptis, P., Kazadzis, S., Eleftheratos, K., Kosmopoulos, P., Amiridis, V., Helmis, C., and Zerefos, C.: Total ozone column measurements using an ultraviolet multifilter radiometer, *International Journal of Remote Sensing*, **2015**, 36(17), 4469–4482, doi: 10.1080/01431161.2015.1083631.

46. Diémoz, H., Eleftheratos, K., Kazadzis, S., Amiridis, V., and Zerefos, C. S.: Retrieval of aerosol optical depth in the visible range with a Brewer spectrophotometer in Athens, *Atmos. Meas. Tech.*, **2016,** 9, 1871–1888, https://doi.org/10.5194/amt-9-1871-2016.

47. Zerefos, C. S., Eleftheratos, K., Kapsomenakis, J., Solomos, S., Inness, A., Balis, D., Redondas, A., Eskes, H., Allaart, M., Amiridis, V., Dahlback, A., De Bock, V., Diémoz, H., Engelmann, R., Eriksen, P., Fioletov, V., Gröbner, J., Heikkilä, A., Petropavlovskikh, I., Jarosławski, J., Josefsson, W., Karppinen, T., Köhler, U., Meleti, C., Repapis, C., Rimmer, J., Savinykh, V., Shirotov, V., Siani, A. M., Smedley, A. R. D., Stanek, M., and Stübi, R.: Detecting volcanic sulfur dioxide plumes in the Northern Hemisphere using the Brewer spectrophotometers, other networks, and satellite observations, *Atmospheric Chemistry and Physics*, , **2017** 17, 551-574, doi: 10.5194/acp-17-551-2017.

48. Gröbner, J. and Meleti, C.: Aerosol optical depth in the UVB and visible wavelength range from Brewer spectrophotometer direct irradiance measurements: 1991–2002, *J. Geophys. Res.*, , **2004** 109, D09202, doi:10.1029/2003JD004409.

49. Staehelin, J., Kerr, J., Evans, R. and Vanicek, K.,. Comparison of total ozone measurements of Dobson and Brewer spectrophotometers and recommended transfer functions. *World Meteorological Organization. Global Atmosphere Watch*, **2003**,*149*.

50. http://www.o3soft.eu/o3brewer.html, access on 10/08/2020

51. Bhartia, P.K. and Wellemeyer, C., TOMS-V8 total O3 algorithm. *OMI Algorithm Theoretical Basis Document*, **2002**, *2*, pp.15-31.

52. Veefkind, J.P., de Haan, J.F., Brinksma, E.J., Kroon, M. and Levelt, P.F., Total ozone from the Ozone Monitoring Instrument (OMI) using the DOAS technique. *IEEE transactions on geoscience and remote sensing*, **2006**,*44*(5), pp.1239-1244.

53. Huijnen, V., Miyazaki, K., Flemming, J., Inness, A., Sekiya, T. and Schultz, M.G., An intercomparison of tropospheric ozone reanalysis products from CAMS, CAMS interim, TCR-1, and TCR-2. *Geoscientific Model Development*, **2020**,*13*(3).

54. B. Mayer and A. Kylling. Technical note: The libRadtran software package for radiative transfer calculations - description and examples of use. *Atmos. Chem. Phys*, **2005.**, 5: 1855-1877

55. C. Emde, R. Buras-Schnell, A. Kylling, B. Mayer, J. Gasteiger, U. Hamann, J. Kylling, B. Richter, C. Pause, T. Dowling, and L. Bugliaro. The libradtran software package for radiative transfer calculations (version 2.0.1). *Geoscientific Model Development* , **2016**, 9(5):1647-1672

56. Raptis, P.-I., Kazadzis, S., Eleftheratos, K., Amiridis, V., and Fountoulakis, I.: Single scattering Albedo's spectral dependence effect on UV irradiance, *Atmosphere*, **2018**, 9, 364, doi:10.3390/atmos9090364.

57. Kazadzis, S., Raptis, P., Kouremeti, N., Amiridis, V., Arola, A., Gerasopoulos, E. and Schuster, G.L., Aerosol absorption retrieval at ultraviolet wavelengths in a complex environment. *Atmospheric Measurement Techniques*, **2016**, *9*(12), p.5997.

58. Plumb, R. A., and J. Eluszkiewicz,: The Brewer–Dobson Circulation: Dynamics of the Tropical Upwelling. *J. Atmos. Sci.*, **1999,** 56, 868–890, https://doi.org/10.1175/1520-0469(1999)056<0868:TBDCDO>2.0.CO;2.

59. Sato, K. and Hirano, S.: The climatology of the Brewer–Dobson circulation and the contribution of gravity waves, *Atmos. Chem. Phys.*, **2019**, 19, 4517–4539, https://doi.org/10.5194/acp-19-4517-2019.

60. Butchart, N., Scaife, A.A., Bourqui, M., De Grandpré, J., Hare, S.H.E., Kettleborough, J., Langematz, U., Manzini, E., Sassi, F., Shibata, K. and Shindell, D., Simulations of anthropogenic change in the strength of the Brewer–Dobson circulation. *Climate Dynamics*, **2006**, *27*(7-8), pp.727-741.